Dynamical Casimir effect for a massless scalar field between two concentric spherical shells with mixed boundary conditions

F. Pascoal,[1] L. C. Céleri,[2] S. S. Mizrahi,[3] M. H. Y. Moussa,[1] and C. Farina[4]

[1]*Instituto de Física, Universidade de São Paulo, Caixa Postal 369, 13566-590 São Carlos, SP, Brazil*
[2]*Centro de Ciências Naturais e Humanas, Universidade Federal do ABC, R. Santa Adélia 166, Santo André 09210-170, SP, Brazil*
[3]*Departamento de Física, Universidade Federal de São Carlos, Via Washington Luis, km 235, São Carlos 13565-905, SP, Brazil*
[4]*Instituto de Física, Universidade Federal do Rio de Janeiro, Caixa Postal 68528, 21945-970 Rio de Janeiro, RJ, Brazil*

In this work we analyze the dynamical Casimir effect for a massless scalar field confined between two concentric spherical shells considering mixed boundary conditions. We thus generalize a previous result in literature [Phys. Rev. A **78**, 032521 (2008)], where the same problem is approached for the field constrained to the Dirichlet-Dirichlet boundary conditions. A general expression for the average number of particle creation is deduced considering an arbitrary law of radial motion of the spherical shells. This expression is then applied to harmonic oscillations of the shells, and the number of particle production is analyzed and compared with the results previously obtained under Dirichlet-Dirichlet boundary conditions.

I. INTRODUCTION

Since the pioneering paper published by Moore in 1970 [1] and the contributions by Fulling and Davies [2] and by Ford and Vilenkin [3] that appeared some years later, radiation reaction force on moving boundaries attracted the attention of many physicists. Due to the movement of the boundary, this topic is also referred to as the dynamical Casimir effect (DCE), a name coined by J. Schwinger in his attempt to explain sonoluminescence in the early 1990s [4]. For a review on this subject see the book by Milton [5] and on DCE see Refs. [6,7].

Though the Casimir force on a unique static plate in vacuum is zero [9], the fluctuations of this force are nonvanishing [8]. Hence, if this plate starts moving with a nonzero general acceleration, we expect that a dissipative force proportional to these fluctuations appears [10–12], and arguments based on energy conservation lead directly to real particle creation.

Though the DCE already occurs for a unique moving boundary, oscillating cavities in parametric resonance with a particular field mode of the corresponding static cavity may enhance significantly the particle creation rate [13–15]. This effect was studied by several authors considering the case of the 1+1 ideal cavity [13,15]. The 3+1 case was also investigated, and different geometries were taken into account, among them parallel plane plates [13,14,16], cylindrical [17], and spherical [18–21] cavities. The nonideal case was also considered in Refs. [22,23].

Concerning the static scenario, Boyer [24] was the first to consider the case of mixed boundary conditions (BCs). He demonstrated that the electromagnetic Casimir force between a perfectly conducting plate and an infinitely permeable one is repulsive rather than attractive. An analogous result was also obtained in the case of a scalar field confined within two parallel plates [25–27] and submitted to a Dirichlet BC at one plate and to a Neumann BC at the other.

The measurement of a repulsive Casimir effect has been pursued for many years and has finally been achieved very recently by Munday, Capasso, and Parsegian [28] in a remarkable experiment involving three distinct media, with appropriate values for their permittivity. Although the setup used by these authors in their experiment on repulsive Casimir effect is quite different from the two-plate setup made of a perfectly conducting plate and an infinitely permeable one, we may learn many things studying the DCE with such mixed BCs. Further, though mixed BCs are relatively common in the study of the static Casimir effect [25–27,29–32], and also in correlated topics of Cavity QED [33–36], the same does not occur for the DCE. In fact, as far as we know, the DCE in a 1+1 dimensional resonant cavity with mixed BCs was considered only very recently, in Refs. [37,38]. However, mixed BCs have never been considered in the study of DCE for different geometries as, for instance, in concentric (and oscillating) spherical shells.

In a recent paper [21], the DCE was examined for a massless scalar field submitted to Dirichlet BCs at two concentric spherical shells, each of them possessing a time-dependent radius. A general expression for the average number of created particles was derived for arbitrary laws of radial motions of the spherical shells. Such an expression was thus applied to breathing modes of the concentric shells: when only one of the shells oscillates and when both shells oscillate in or out of phase. The purpose of this paper is to complement the previous one [21] by considering mixed BCs. We observe that the field modes associated with mixed BCs differs from that following from Dirichlet-Dirichlet (DD) BCs. Our calculations constitutes preliminary (and much simpler) results that enlighten the more realistic problem involving the electromagnetic field. The reason for that is explained in what follows.

Let us admit the Casimir effect, where a quantum electromagnetic field is constrained between two static infinitely conducting parallel plates, where the Coulomb gauge is assumed. The decomposition into TE and TM modes can be implemented with two scalar fields, ϕ and ψ, where ϕ (ψ) is submitted to DD (Neumann-Neumann, NN) BC at both plates. The frequencies for ϕ and ψ are

$$\omega^{(\mathrm{DD})}(k_x, k_y, n) = c\sqrt{k_x^2 + k_y^2 + \frac{n^2\pi^2}{a^2}}, \quad n = 1, 2, \ldots,$$

$$\omega^{(\mathrm{NN})}(k_x, k_y, n) = c\sqrt{k_x^2 + k_y^2 + \frac{n^2\pi^2}{a^2}}, \quad n = 0, 1, 2, \ldots,$$

with the plates located at $z = 0$ and $z = a$, respectively. Except for the term $n = 0$ in the NN case, all frequencies are the same in the above equations. However, this term is not important in the computation of the Casimir effect since it does not depend on the distance a between the plates. Hence, in order to compute the Casimir energy of the electromagnetic field between two parallel perfectly conducting plates, we can simply compute the Casimir effect for a massless scalar field submitted to DD BC at both plates and multiply the final result by 2.

We next assume the Casimir effect for the quantum electromagnetic field constrained between an infinitely conducting plate at $z = 0$ and an infinitely permeable one at $z = a$ [24]. The decomposition into TE and TM modes can still be easily implemented with two scalar fields, ϕ and ψ, where ϕ is submitted to Dirichlet BC at $z = 0$ and Neumann BC at $z = a$, whereas ψ is submitted to Neumann BC at $z = 0$ and Dirichlet BC at $z = a$. For both cases, the frequencies of the field modes are

$$\omega^{(\mathrm{DN})}(k_x, k_y, n) = \omega^{(\mathrm{ND})}(k_x, k_y, n)$$
$$= c\sqrt{k_x^2 + k_y^2 + \frac{\left(n + \frac{1}{2}\right)^2\pi^2}{a^2}}, \quad n$$
$$= 0, 1, 2, \ldots.$$

In order to compute the Casimir energy of the electromagnetic field between a perfectly conducting plate and an infinitely permeable one, we can simply compute the Casimir effect for a massless scalar field submitted to mixed BC, namely, Dirichlet BC at one plate and Neumann BC at the other, and again multiply the final result by 2.

The arguments given above explain the great interest in making Casimir calculations involving mixed boundary conditions. The formal treatment of the dynamical Casimir effect for the electromagnetic field inside two concentric spherical shells, with radial oscillations, is much more involved. However, since in some appropriate limit, spherical shells reduce to parallel plates, it is reasonable to analyze the physical scenario involving the simpler problem of a massless scalar field inside two concentric spherical shells submitted to mixed BCs.

Therefore, considering the oscillatory motion of the shells as assumed in Ref. [21], in the present contribution we identify all the resonances under mixed BCs and derive the expression for the associated particle creation rate. Then, performing a numerical analysis we compare our results with those presented in Ref. [21]. For convenience, we shall assume that the spherical shell on which we impose Neumann BC is at rest, while the other, on which we impose Dirichlet BC is in an arbitrary motion. We shall study two situations: when the inner shell is at rest while the outer undergoes an

arbitrary motion, and the reverse case with the outer shell at rest and the inner in arbitrary motion. Comparisons of our results with those involving only DD BCs are presented graphically.

This paper is organized as follows: in Sec. II we briefly summarize the main steps of the method employed to the case where only Dirichlet BCs were considered. in Sec. III we apply this method to the case of mixed BCs and obtain our general formulas. With the purpose of obtaining explicit results for the average number of created particles, in Sec. IV we choose a particular motion for the oscillating shell. Section V is left for the concluding remarks.

II. DIRICHLET-DIRICHLET BCS

In Ref. [21] the DCE for a massless scalar field confined between two concentric moving shells was considered. This quantum scalar field obeys the Klein-Gordon equation $\Box\phi(\mathbf{r};t) = 0$. Besides, this field and its canonical momentum $\pi(\mathbf{r};t) = \dot{\phi}(\mathbf{r};t)$ satisfy the equal time commutation relations

$$[\phi(\mathbf{r};t), \pi(\mathbf{r}';t)] = i\delta(\mathbf{r} - \mathbf{r}'),$$

$$[\phi(\mathbf{r};t), \phi(\mathbf{r}';t)] = [\pi(\mathbf{r};t), \pi(\mathbf{r}';t)] = 0. \quad (1)$$

The spherical symmetry of the problem leads us to the following solution:

$$\phi(\mathbf{r};t) = \sum_{l=0}^{\infty}\sum_{m=-l}^{l}\sum_{s=1}^{\infty}\sqrt{\frac{1}{2\omega_{ls}(t)}}F_{ls}(r;t)[a_{lms}(t)Y_{lm}(\theta,\varphi)$$
$$+ \mathrm{H.c.}],$$

$$\pi(\mathbf{r};t) = -i\sum_{l=0}^{\infty}\sum_{m=-l}^{l}\sum_{s=1}^{\infty}\sqrt{\frac{\omega_{ls}(t)}{2}}F_{ls}(r;t)[a_{lms}(t)Y_{lm}(\theta,\varphi)$$
$$- \mathrm{H.c.}], \quad (2)$$

where $\{Y_{lm}(\theta,\varphi)\}$ are the spherical harmonics and the orthonormal radial functions satisfy the following differential equation

$$\frac{1}{r^2}\frac{d}{dr}\left(r^2\frac{dF_{ls}(r;t)}{dr}\right) + \left(\frac{\omega_{ls}^2(t)}{c^2} - \frac{l(l+1)}{r^2}\right)F_{ls}(r;t) = 0. \quad (3)$$

Moreover, the operators $a_{lms}(t)$ and $a_{lms}^{\dagger}(t)$ obey the standard commutation relations

$$[a_{lms}(t), a_{l'm's'}^{\dagger}(t)] = \delta_{ll'}\delta_{mm'}\delta_{ss'},$$

$$[a_{lms}(t), a_{l'm's'}(t)] = [a_{lms}^{\dagger}(t), a_{l'm's'}^{\dagger}(t)] = 0. \quad (4)$$

Through the time derivative of Eqs. (2), together with the Klein-Gordon equation and the canonical momentum formula, we obtain the time evolution for the operators

$$\dot{a}_{lms}(t) = -i\omega_{ls}(t)a_{lms}(t) + \sum_{s'}\mu_{l[ss']}(t)a_{lms'}(t) + \sum_{s'}\mu_{l(ss')}$$
$$\times(t)a_{l(-m)s'}^{\dagger}(t), \quad (5)$$

where the functions $\mu_{l(ss')}(t) = [\mu_{lss'}(t) + \mu_{ls's}(t)]/2$ and

$\mu_{l[ss']}(t) = [\mu_{lss'}(t) - \mu_{ls's}(t)]/2$ are the symmetric and anti-symmetric parts, respectively, of the time-dependent coefficient

$$\mu_{lss'}(t) = \frac{\dot{\omega}_{ls}(t)}{2\omega_{ls}(t)}\delta_{ss'} + (1$$
$$- \delta_{ss'})\sqrt{\frac{\omega_{ls}(t)}{\omega_{ls'}(t)}}\int_{r_i(t)}^{r_o(t)} r^2 F_{ls'}(r;t)\dot{F}_{ls}(r;t)\mathrm{d}r. \quad (6)$$

As demonstrated in Ref. [21], by comparing Eq. (5) with the Heisenberg equation of motion $\dot{a}_{lms}(t) = i[H_{\mathrm{eff}}(t), a_{lms}(t)]$ and assuming the most general quadratic form of an effective Hamiltonian, we derive

$$H_{\mathrm{eff}}(t) = \sum_{l,m,s} \omega_{ls}(t)\left(a_{lms}^\dagger a_{lms} + \frac{1}{2}\right) + \frac{i}{2}\sum_{l,m,s,s'} \mu_{lss'}(t)[(a_{lms'}$$
$$+ a_{l(-m)s'}^\dagger)a_{lms}^\dagger - a_{lms}(a_{l(-m)s'} + a_{lms'}^\dagger)]. \quad (7)$$

The evolution of the density operator is computed through the relation $\dot{\rho}(t) = i[H_{\mathrm{eff}}(t), \rho(t)]$, with the aid of an iterative procedure up to second-order approximation in the velocity of the cavity boundaries, i.e., $\dot{r}_i(t)$, $\dot{r}_0(t) \ll c$. The derivation of the average number of particles created in a particular mode—labeled by the quantum numbers (l, m, s)—is thus given by $\mathcal{N}_{lms}(t) = \mathrm{Tr}[\rho(t)a_{lms}^\dagger(0)a_{lms}(0)]$, and for an initial vacuum state $\rho(0) = |\{0\}\rangle|\{0\}\rangle$ it follows that

$$\mathcal{N}_{lms}(t) = \sum_{s'} \left| \int_0^t \mathrm{d}t_1 \mu_{l(s's)}(t_1)\exp\{i[\Omega_{ls'}(t_1) + \Omega_{ls}(t_1)]\} \right|^2,$$
$$(8)$$

with $\Omega_{ls}(t) = \int_0^t dt_1 \omega_{ls}(t_1)$.

The number of created particles $\mathcal{N}_{lms}(t)$ depends on the radial function $F_{ls}(r;t)$ through $\mu_{l(s's)}(t)$. The solution of Eq. (3) is given by a linear combination of spherical Bessel functions of the first (j_l) and second (n_l) kind, such that the Dirichlet BC applied to the inner shell leads to the relation

$$F_{ls}(r;t) = N_{ls}\{j_l[\omega_{ls}(t)r]n_l[\omega_{ls}(t)r_i] - j_l[\omega_{ls}(t)r_i]n_l[\omega_{ls}(t)r]\},$$
$$(9)$$

whereas that on the outer shell results in the transcendental equation

$$j_l[\omega_{ls}(t)r_o]n_l[\omega_{ls}(t)r_i] - j_l[\omega_{ls}(t)r_i]n_l[\omega_{ls}(t)r_o] = 0. \quad (10)$$

In Fig. 1 we present a map of the solutions of Eq. (10) for some values of the numbers l and s. As it was noted in [21], for the case $l=0$, the frequencies are equally spaced. This fact does not occur for the case $l \neq 0$. However, when both radii of the shells are much larger than the separation between them, i.e., $r_i(t) \gg r_o(t) - r_i(t)$, the solutions for all values of l approach the solution for the one-dimensional case, so that $\omega_{ls} \to s\pi/[r_o(t) - r_i(t)]$.

III. MIXED BOUNDARY CONDITIONS

It is important to emphasize that the expression for the average number of created particles, derived in Eq. (8), does
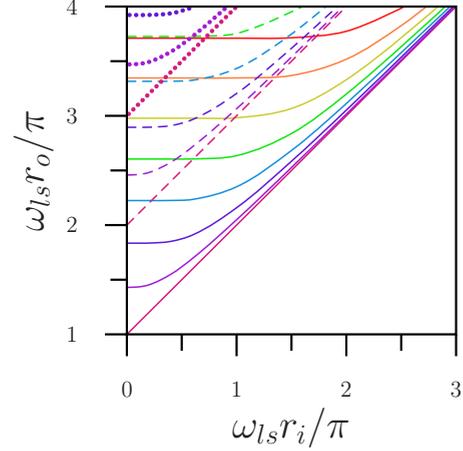

FIG. 1. (Color online) Map of the solutions of the transcendental Eq. (10). The colors correspond to different values of the number l in ascending order from zero. The solid, dashed, and dotted lines correspond to $s=1$, $s=2$, and $s=3$, respectively.

not depend on the character of the BCs. Thus it can be applied even for mixed BCs as in the present work, where we assume that the massless scalar field satisfies the Neumann BC at a fixed spherical shell and a Dirichlet BC at a second concentric spherical shell whose radius has an arbitrary time dependence,

$$\partial_r \phi(\mathbf{r},t)|_{r=r_\alpha} = 0 \quad \text{and} \quad \phi(\mathbf{r},t)|_{r=r_\beta(t)} = 0, \quad (11)$$

where the index $\alpha(\beta)$ is related to the static (moving) shell. However, different expressions come up for $F_{ls}(r;t)$ and $\omega_{ls}(t)$, as compared to those in Ref. [17].

As already noted in the previous section, the general solutions to Eq. (3) are linear combinations of spherical Bessel functions, but the mixed BC leads to a different solution. The assumption of Neumann BC for the field at the static shell leads to the following expression for the radial functions

$$F_{ls}(r;t) = N_{ls}\left\{j_l[\omega_{ls}(t)r]\frac{\partial}{\partial r_\alpha}n_l[\omega_{ls}(t)r_\alpha]\right.$$
$$\left. - n_l[\omega_{ls}(t)r]\frac{\partial}{\partial r_\alpha}j_l[\omega_{ls}(t)r_\alpha]\right\}, \quad (12)$$

and the subsequent assumption of Dirichlet BC on the field at the moving shell leads to a frequency discretization

$$\frac{\partial}{\partial r_\alpha}j_l[\omega_{ls}(t)r_\alpha]n_l[\omega_{ls}(t)r_\beta(t)] = j_l[\omega_{ls}(t)r_\beta(t)]\frac{\partial}{\partial r_\alpha}n_l[\omega_{ls}(t)r_\alpha].$$
$$(13)$$

In Figs. 2 and 3 we show the maps of the numerical solutions of the transcendental equation Eq. (13) for some values of l and s. As we can see, the map of $\omega_{ls}(t)$ is very sensitive to the BCs. For DD BCs (Fig. 1) the frequencies $\omega_{0s}(t)$ are equally spaced, a situation that does not occur for mixed BCs. We also note that the map of $\omega_{ls}(t)$ turns out to
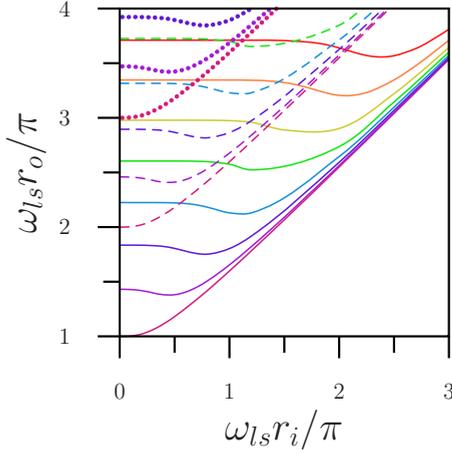
$$\partial_{r'}\phi(\mathbf{r}',t)|_{r'=r_\beta(t)} \Rightarrow \{\partial_r + \dot{r}_\beta(t)\partial_t\}\phi(\mathbf{r},t)|_{r=r_\beta(t)} = 0. \quad (14)$$

In that case, the time derivative in Eq. (14) invalidates the expansion used in Eq. (2), and as a consequence, also in Eq. (8). This fact demands a different formal development for the computation of the required particle creation rate. For that reason, in the present work we treat only the case where the Neumann BC is imposed on a spherical shell at rest, leaving aside the breathing modes analyzed in Ref. [21], when both shells oscillate in or out of phase.

IV. NUMERICAL ESTIMATIVES

In this section, in order to obtain explicit results, we will consider an specific motion for the spherical shell that imposes on the field the Dirichlet BC. A typical situation consists of an oscillation that starts at some instant has a sinusoidal behavior with an angular frequency ϖ and a small amplitude and then stops at some later instant. We, then, assume that the radius of the moving shell has the following law of motion:

$$r_\beta(t) = r_\beta[1 + \epsilon \sin(\varpi t)], \quad (15)$$

with $\epsilon \ll 1$. In the following we also assume that the cavity mirror oscillates only during a finite time interval T, then stopping suddenly its motion.

Substituting Eqs. (6) and (15) into Eq. (8) and making a power series expansion with respect to the small parameter ϵ, we obtain

$$\mathcal{N}_{lms} = \left(\frac{\epsilon\varpi T}{2}\right)^2 \sum_{s'} |C_{l(ss')}f_{lss'}(\varpi;T)|^2, \quad (16)$$

where, after defining $\omega_{lss'} \equiv \omega_{ls}(0) + \omega_{ls'}(0)$, the coefficient $C_{lss'}$ and function $f_{lss'}(\varpi;T)$ are given by

$$f_{lss'}(\varpi;T) = \frac{\exp[i(\varpi - \omega_{lss'})T] - 1}{i(\varpi - \omega_{lss'})T}$$
$$- \frac{\exp[-i(\varpi + \omega_{lss'})T] - 1}{i(\varpi + \omega_{lss'})T}, \quad (17)$$

and

$$C_{lss'} = r_\beta \delta_{ss'} \frac{1}{2\omega_{ls}(0)} \frac{\partial \omega_{ls}(0)}{\partial r_\beta} - r_\beta(1$$
$$- \delta_{ss'})\sqrt{\frac{\omega_{ls}(0)}{\omega_{ls'}(0)}} \int_{r_i}^{r_o} dr r^2 F_{ls}(r;0) \frac{dF_{ls'}(r;0)}{dr_\beta}. \quad (18)$$

Note that $f_{lss'}(\varpi;T)$ is an oscillating function of T, except when the mirror oscillating frequency satisfies the resonance condition, namely, $\varpi = \omega_{lss'}$. In this case $f_{lss'}(\omega_{lss'};T) = 1$, and the number of created particles turns to be the following quadratic function of T:

FIG. 2. (Color online) Map of the solutions of the transcendental Eq. (13) with $r_\alpha < r_\beta$. The colors correspond to different values of the number l in ascending order from zero. The solid, dashed, and dotted lines correspond to $s=1$, $s=2$, and $s=3$, respectively.

be entirely different when considering the Dirichlet BC in the outer shell and Neumann BC in the inner one (Fig. 2) or oppositely, with Neumann BC in the outer shell and Dirichlet BC in the inner one (Fig. 3).

However, there are also some similarities between the results derived from mixed BCs and those for DD BCs, in Fig. 1; it can be directly verified that the solutions for $\omega_{ls}(t)$, coming from Eq. (13), approach that for the one-dimensional case $(\omega_{ls} \to (s-1/2)\pi/|r_\alpha - r_\beta(t)|)$ when both radii of the shells are much larger than the separation between them.

A comment is in order here: we note that the BCs must be imposed in the instantaneously comoving Lorentz frame, where the boundaries are momentarily at rest. If the Neumann BC was to be imposed on the moving boundary, we should have used the appropriate Lorentz transformation to write the fields in the inertial frame of the laboratory as follows
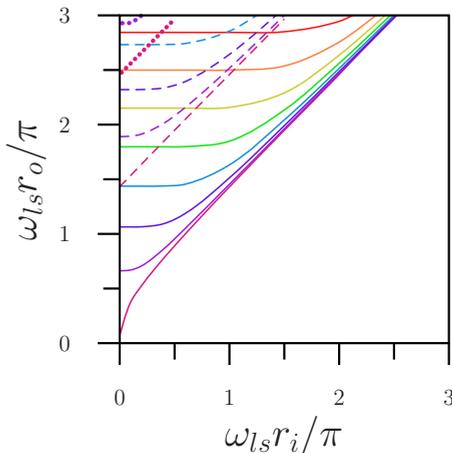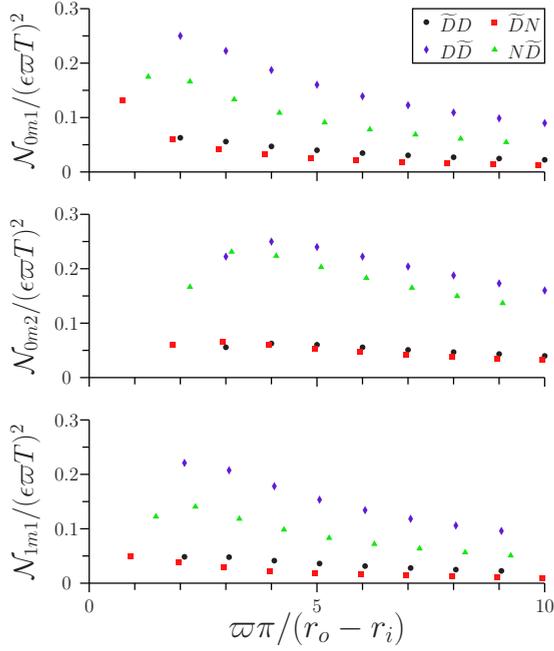

FIG. 3. (Color online) Map of the solutions of the transcendental Eq. (13) with $r_\alpha > r_\beta$. The colors correspond to different values of the number l in ascending order from zero. The solid, dashed, and dotted lines correspond to $s=1$, $s=2$, and $s=3$, respectively.

FIG. 4. (Color online) Plot of $\mathcal{N}_{lms}/(\epsilon\varpi T)^2$ as a function of $\varpi\pi/(r_o-r_i)$, in the resonance condition for a few values of l and s. We have considered DD and Mixed BCs. On the legend (top-right of the figure), the letter on the left indicates the BC imposed on the field at the inner shell and the letter to the right, indicates the BC imposed on the field at the outer shell. D means Dirichlet BC and static shell, $\widetilde{D}$ means Dirichlet BC and moving shell, whereas N means Neumann BC and static shell. We have set $r_o=2r_i$.

$$\lim_{\omega\to\omega_{lss'}} \mathcal{N}_{lms} = \left(\frac{\epsilon\omega_{lss'}T}{2}\right)^2 |C_{l(ss')}|^2. \qquad (19)$$

This result is valid only under the short-time approximation $\epsilon\omega_{lss'}T \ll 1$, since we have disregard terms proportional to $(\epsilon\omega_{lss'}T)^n$ with $n \geq 3$. Moreover, Eqs. (16)–(19) are valid either for DD BCs or mixed BCs since they were derived using the equation of motion [Eq. (15)] and Eqs. (1)–(8) which are independent from the BCs.

To study the behavior of our result in Eq. (19), we plot in Fig. 4 the expression $\mathcal{N}_{lms}/(\epsilon\varpi T)^2$ as a function of $\varpi\pi/(r_o-r_i)$ for some values of l and s, under resonance conditions $\varpi=\omega_{lss'}$, setting $r_o=2r_i$. Both letters in the legend indicate the BCs on the inner and the outer shells, respectively: for example, $D(\widetilde{D})$ means Dirichlet BC on a static (moving) shell, whereas N means Neumann BC on a static shell. As we can see, both the intensity and position of the resonances change in a nontrivial way with the BC. The case of a moving outer shell with the field satisfying DD BCs exhibits higher resonance intensities, while the case of a moving inner shell with the field submitted to mixed BCs leads to lower resonance frequencies.

In the limit $r_i \gg r_o-r_i$, we can use the Bessel asymptotic forms for large arguments to derive an analytical expression for the average number of created particles in a particular mode. For the case where the field is submitted to DD BCs, we obtain

$$\omega_{lss'} \to \frac{(s+s')\pi}{|r_\alpha - r_\beta|} \qquad (20)$$

and

$$\lim_{\omega\to\omega_{lss'}} \mathcal{N}_{lms} \to \frac{\epsilon^2\pi^2 T^2}{4}\frac{r_\beta^2}{(r_\alpha-r_\beta)^4}s's. \qquad (21)$$

Analogously, for the field submitted to mixed BCs [Eq. (11)], we have

$$\omega_{lss'} \to \frac{(s+s'-1)\pi}{|r_\alpha - r_\beta|} \qquad (22)$$

and

$$\lim_{\omega\to\omega_{lss'}} \mathcal{N}_{lms} \to \frac{\epsilon^2\pi^2 T^2}{16}\frac{r_\beta^2}{(r_\alpha-r_\beta)^4}(2s'-1)(2s-1). \qquad (23)$$

Expressions (20) and (21) correspond to the results for the 1+1 DCE under DD BCs derived in Refs. [6,13,15], whereas Eqs. (22) and (23) correspond to the results under mixed BCs presented in [25–27]. These similarities can be related to the fact that the limit $r_i \gg r_o-r_i$ is akin to the plane geometry.

V. CONCLUDING REMARKS

In this paper we have investigated the dynamical Casimir effect for a massless scalar field within two concentric spherical shells considering mixed boundary conditions. We have thus complemented some previous results presented in Ref. [21] where the massless scalar field was assumed to satisfy only Dirichlet BC in both shells. We have analyzed the real particle creation phenomenon for the case where only one of the shells is allowed to move with an arbitrary law of motion for its radius. In addition, the Dirichlet BC was imposed on the moving shell while the Neumann's was assumed on the static one. However, in our discussion, the moving shell could be the inner shell or the outer one as well. In order to get some numerical estimatives, and with the purpose of comparing our results with those obtained in Ref. [21], we chose a particular, but very typical, oscillating motion for the moving shell, in which it starts moving at a certain instant, oscillates with a given frequency and then stops suddenly its motion. Considering this particular situation, we have identified the resonance conditions where the number of created particles is more appreciable. A direct inspection in our graphs (see Fig. 4), allows us to make some conclusions: for both cases of DD BCs or mixed BCs, we see that every time the moving shell is the outer one the average number of created particles is greater than the corresponding cases where the inner shell is in motion (by a factor of the order of ~4). This can be understood simply recalling that the dynamical Casimir effect increases with the area of the moving surface. In other words, the dissipative force that acts on the moving boundary, responsible for converting mechanical energy into field energy (real field *quanta*) increases with the area with the moving boundary. Another interesting result that can be extracted from our calculations is the fact that the case with mixed BCs presents lower resonance fre-

quencies than that with DD BCs. This feature can be useful for further experimental investigations of particle creation within the context of the dynamical Casimir effect since it makes easier to access the parametric amplification regime of particle creation.

[1] G. T. Moore, J. Math. Phys. **11**, 2679 (1970).

[2] S. A. Fulling and P. C. W. Davies, Proc. R. Soc. London, Ser. A **348**, 393 (1976).

[3] L. H. Ford and A. Vilenkin, Phys. Rev. D **25**, 2569 (1982).

[4] J. Schwinger, Proc. Natl. Acad. Sci. U.S.A. **90**, 2105 (1993).

[5] K. A. Milton, *Physical Manifestation of Zero Point Energy— The Casimir Effect* (World Scientific, Singapore, 2001).

[6] V. V. Dodonov, in *Modern Nonlinear Optics*, Advances in Chem. Phys. Series Vol. 119, edited by M. W. Evans (Wiley, New York, 2001) p. 309.

[7] A. Lambrecht, J. Opt. B: Quantum Semiclassical Opt. **7**, S3 (2005).

[8] G. Barton. J. Phys. A **24**, 991 (1991); **24**, 5533 (1991).

[9] H. Nyquist, Phys. Rev. **32**, 110 (1928); H. B. Callen and T. A. Welton, *ibid.* **83**, 34 (1951); R. Kubo, Rep. Prog. Phys. **29**, 255 (1966).

[10] V. B. Braginsky and F. Ya. Khalili, Phys. Lett. A **161**, 197 (1991).

[11] M.-T. Jackel and S. Reynaud, Quantum Opt. **4**, 39 (1992).

[12] P. A. Maia-Neto and S. Reynaud, Phys. Rev. A **47**, 1639 (1993).

[13] V. V. Dodonov and A. B. Klimov, Phys. Rev. A **53**, 2664 (1996).

[14] A. Lambrecht, M.-T. Jaekel, and S. Reynaud, Phys. Rev. Lett. **77**, 615 (1996).

[15] J.-Y. Ji, H.-H. Jung, and K.-S. Soh, Phys. Rev. A **57**, 4952 (1998).

[16] D. F. Mundarain and P. A. Maia Neto, Phys. Rev. A **57**, 1379 (1998).

[17] M. Crocce, D. A. R. Dalvit, F. C. Lombardo, and F. D. Mazzitelli, J. Opt. B: Quantum Semiclassical Opt. **7**, S32 (2005).

[18] C. Eberlein, Phys. Rev. Lett. **76**, 3842 (1996).

[19] M. R. Setare and A. A. Saharian, Mod. Phys. Lett. A **16**, 927 (2001).

[20] F. D. Mazzitelli and X. O. Millan, Phys. Rev. A **73**, 063829 (2006).

[21] F. Pascoal, L. C. Céleri, S. S. Mizrahi, and M. H. Y. Moussa, Phys. Rev. A **78**, 032521 (2008).

[22] G. Schaller, R. Schützhold, G. Plunien, and G. Soff, Phys. Rev. A **66**, 023812 (2002).

[23] L. C. Céleri, F. Pascoal, M. A. de Ponte, and M. H. Moussa, Ann. Phys (N.Y.) e-print arXiv:0805.0786 (to be published).

[24] T. H. Boyer, Phys. Rev. A **9**, 2078 (1974).

[25] V. Hushwater, Am. J. Phys. **65**, 381 (1997).

[26] M. V. Cougo-Pinto, C. Farina, and A. Tenório, Braz. J. Phys. **29**, 371 (1999).

[27] A. C. Aguiar Pinto, T. M. Britto, R. Bunchaft, F. Pascoal, and F. S. S. Rosa, Braz. J. Phys. **33**, 860 (2003).

[28] J. N. Munday, Federico Capasso, and V. Adrian Parsegian, Nature (London) **457**, 170 (2009).

[29] Xiang-hua Zhai and Xin-zhou Li, Phys. Rev. D **76**, 047704 (2007).

[30] S. A. Fulling, L. Kaplan, and J. H. Wilson, Phys. Rev. A **76**, 012118 (2007).

[31] L. P. Teo, J. Phys. A **42**, 105403 (2009).

[32] E. Elizalde, S. D. Odintsov, and A. A. Saharian, Phys. Rev. D **79**, 065023 (2009).

[33] M. V. Cougo-Pinto, C. Farina, F. Santos, and A. Tort, Phys. Lett. B **446**, 170 (1999).

[34] M. V. Cougo-Pinto, C. Farina, F. Santos, and A. Tort, J. Phys. A **32**, 4463 (1999).

[35] D. T. Alves, C. Farina, and A. C. Tort, Phys. Rev. A **61** 034102 (2000).

[36] D. T. Alves, F. Barone, C. Farina, and A. C. Tort, Phys. Rev. A **67**, 022103 (2003).

[37] D. T. Alves, C. Farina, and E. R. Granhen, Phys. Rev. A **73**, 063818 (2006).

[38] D. T. Alves and E. R. Granhen, Phys. Rev. A **77**, 015808 (2008).